Structural geology and well planning in the Clair Field

STEVEN OGILVIE[1]*, DAVID BARR[2], PAUL ROYLANCE[2] & MATTHEW DORLING[2]

[1]*BP Exploration Ltd, 153 Neftchilar Avenue, Port Baku, N Tower, Baku, AZ1010, Azerbaijan*

[2]*BP Exploration Ltd, 1 Wellheads Avenue, Dyce, Aberdeen AB21 7PB, UK*

**Corresponding author (e-mail: Steven.ogilvie@bp.com)*

Abstract: The Clair Field is a giant oilfield located approximately 70 km west of the Shetland Isles, UK. It was discovered in 1977 and brought on stream some 28 years later. Key to unlocking its economic potential was a series of appraisal wells drilled in the early 1990s that identified fractures as the primary production mechanism. Structural geology contributed in several ways to the detailed planning of the development and appraisal wells. In the sandy (Tertiary) tophole section, outcrop analogues and offset wells were used to establish an appropriate standoff from major faults. This was to mitigate the risk of wellbore instability in what is otherwise a relatively benign sequence to drill. The mid-section, Upper Cretaceous mudstone is prone to wellbore instability, believed to be caused by strength anisotropy with respect to bedding. Here, polygonal faulting may contribute directly to wellbore instability. The associated bed rotation also influences anisotropic failure, which depends in part on the wellbore-to-bedding intersection angle. An example is given of how an understanding of the structural evolution of the overburden section impacts well casing placement. Finally, judgement on the nature of the faulted contact between two fault blocks was required for the pressure prognosis of a planned well.

The Clair Field is a giant oilfield located approximately 70 km west of the Shetland Isles (Fig. 1). It was discovered in 1977 by well 206/8-1A. Devonian-age continental fluvial sandstones form the Lower Clair Group Reservoir. Natural fractures boost the effective permeability, resulting in higher oil production rates than expected from matrix properties alone (Fig. 2). The trap itself is a four-way closure extending over approximately 220 km^2 (Witt *et al.* 2010). The top seal is Upper Cretaceous mudstone.

The early appraisal wells in the Clair Ridge area (Fig. 1b) failed to confirm economically recoverable hydrocarbons. This is because vertical (or near-vertical) wells are unlikely to penetrate many potentially productive open fractures. High-angle appraisal wells in the 1990s penetrated vertical fractures and confirmed that the oil was recoverable. This paved the way for first oil from the Clair Phase 1 (Fig. 1b) platform in 2005. Since then, 19 production wells have been drilled.

Some production wells depend upon open fractures to deliver commercial oil rates. Other wells have penetrated good quality matrix (porosities greater than 15%) and in these cases fractures may assist oil production. Appraisal of the Clair Ridge area commenced in 2005 with high-angle appraisal wells designed to intersect fractures. These modern wells confirmed that the Clair Ridge area could be developed by up to 36 production wells drilled from a dedicated platform. Detailed planning of the early Clair Phase II production wells started in 2009. A more detailed discussion of the development of the Clair Field is given by Witt *et al.* (2010).

This paper outlines how structural geology contributed to the detailed planning of these wells. These issues will be presented in three well sections that are illustrated for a typical high-angle Clair production and appraisal well in Figure 3. Examples will also be given for vertical or inclined appraisal wells. These tend to have the same mid-top section issues as high-angle wells but are not usually targeting reservoir fractures; therefore, they differ in the reservoir section. This paper uses a fracture type classification similar to that described by Gabrielsen & Koestler (1987). The main types of fractures are faults, joints and deformation bands. Faults have had shear displacement whereas joints are opening mode fractures with no evidence of shear displacement. Deformation bands (e.g. Gibson 1998; Fossen *et al.* 2007) have also experienced shear deformation that resulted in grain comminution and porosity collapse. This effect is greatest in high-porosity reservoirs. Polygonal faults (e.g. Cosgrove 1998; Goulty & Swarbrick 2005) with displacements often in the tens of metres range occur in the Upper Cretaceous mudstones (well mid-section). The most prominent set offset a mid-Maastrichtian horizon but are truncated by the base Tertiary unconformity and deeper sets are stratabound within narrow stratigraphic intervals, implying that they formed within a few million

From: Richards, F. L., Richardson, N. J., Rippington, S. J., Wilson, R. W. & Bond, C. E. (eds) 2015. *Industrial Structural Geology: Principles, Techniques and Integration*. Geological Society, London, Special Publications, **421**, 197–212. First published online February 23, 2015, http://dx.doi.org/10.1144/SP421.7

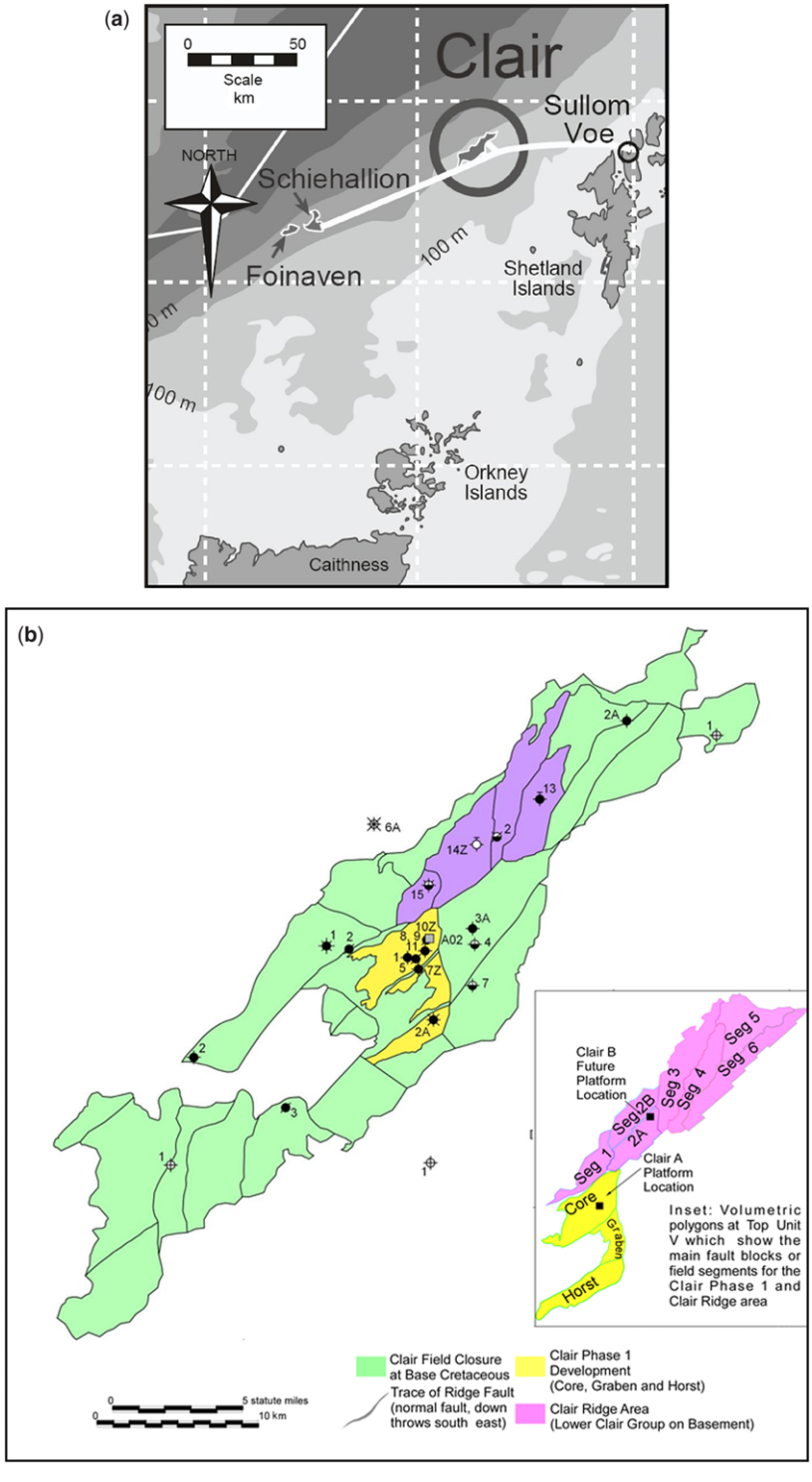

Fig. 1. (**a**) Clair Field location map. The oil column is *c.* 600 m and water depth *c.* 140 m. (**b**) Extent of Clair Field closure showing Clair Phase 1 (yellow segments) and Clair Phase 2 (purple segments).

Fig. 2. Open fractures/joints in Devonian sandstones, Caithness, UK to illustrate the nature of the fracturing penetrated. St Mary's Chapel, Caithness (GR ND 025 702). Photograph courtesy of Alex Milne.

years of deposition and at relatively shallow depth (hundreds of metres).

In Clair, production and high-angle (up to 90° from the vertical) appraisal wells are planned to penetrate as many fractures in the reservoir as possible as the rock matrix may not provide sufficient permeability for hydrocarbon production (Fig. 2 and Barr *et al.* 2007). In order to reach these reservoir targets, it is necessary to minimize contact with seismic-scale faults in the top (Tertiary) and mid (Cretaceous) sections as this may risk wellbore instability. The amount of standoff (distance to stay

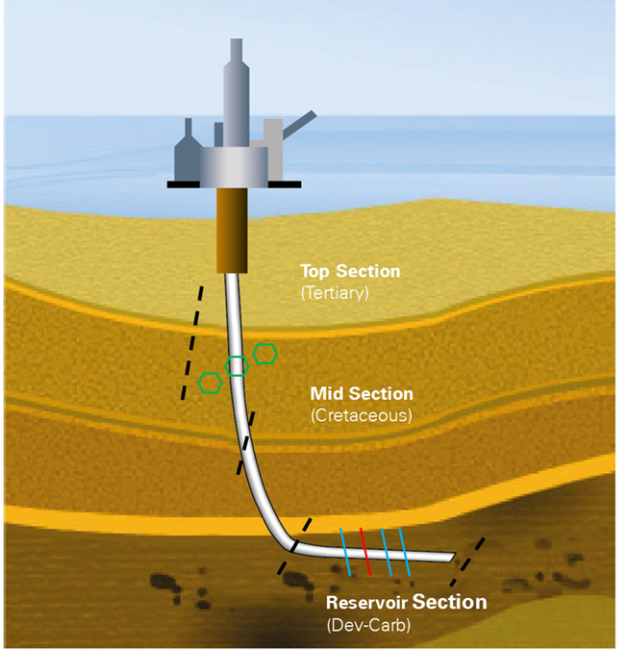

Fig. 3. Structural geology issue by well section. The depth scale is approximately 2000 m total vertical depth (TVD) from top to bottom. Not all issues are discussed in this paper in detail.

Fracture Types

- Faults
- Joints
- Deformation bands
- Polygonal faults

Topic by well section	Issue addressed
Distance to Fault	Wellbore instability
Structural Evolution	Well Placement
Polygonal Faults in Muds	Wellbore instability
Structural Evolution	Well Placement
Faults on Reservoir Entry	Casing shoe placement Stratigraphy count-down
Intersecting joints/seismic faults	Well spacing Reservoir deliverability
Fault Seal	Well Placement Contingency Planning

away from a fault) is therefore a key question during well planning. This requires an understanding of the structural geology in the vicinity of the well path. This is the first example of the role of structural geology in well planning to be discussed in this contribution. A structural geology workflow has been applied to assessing the required standoff in the top section but has also been applied at the toe of the well when devising the well total depth criteria. The second example will be taken from the mid-section of representative wells. Here, the Cretaceous is extensively deformed by polygonal faults. Rock strength anisotropy present in the mudstones makes wellbore stability dependent on wellbore-to-bedding intersection angle. Faults may pose challenges for wellbore stability directly, through infall of unconsolidated fault breccia or, indirectly, by rotating bedding to an adverse intersection angle. Then an example is given where an understanding of the structural geology has impacted well casing placement. Finally, the need for judgement on the likely juxtaposition of rocks of differing ages across a fault between a producing well and a planned well is outlined.

We begin the paper with a summary of the structural history of the field. More details are given by Coney *et al.* (1993), Nichols (2005), Barr *et al.* (2007) and Witt *et al.* (2010).

Clair structural evolution

The Clair Field is located in the southern part of the extensional Faroe–Shetland Basin, which is of Devonian to Cretaceous age (Fig. 4). Clair is bounded to the NW by Rona Ridge Fault system and to the SE by the West Shetland Basin and

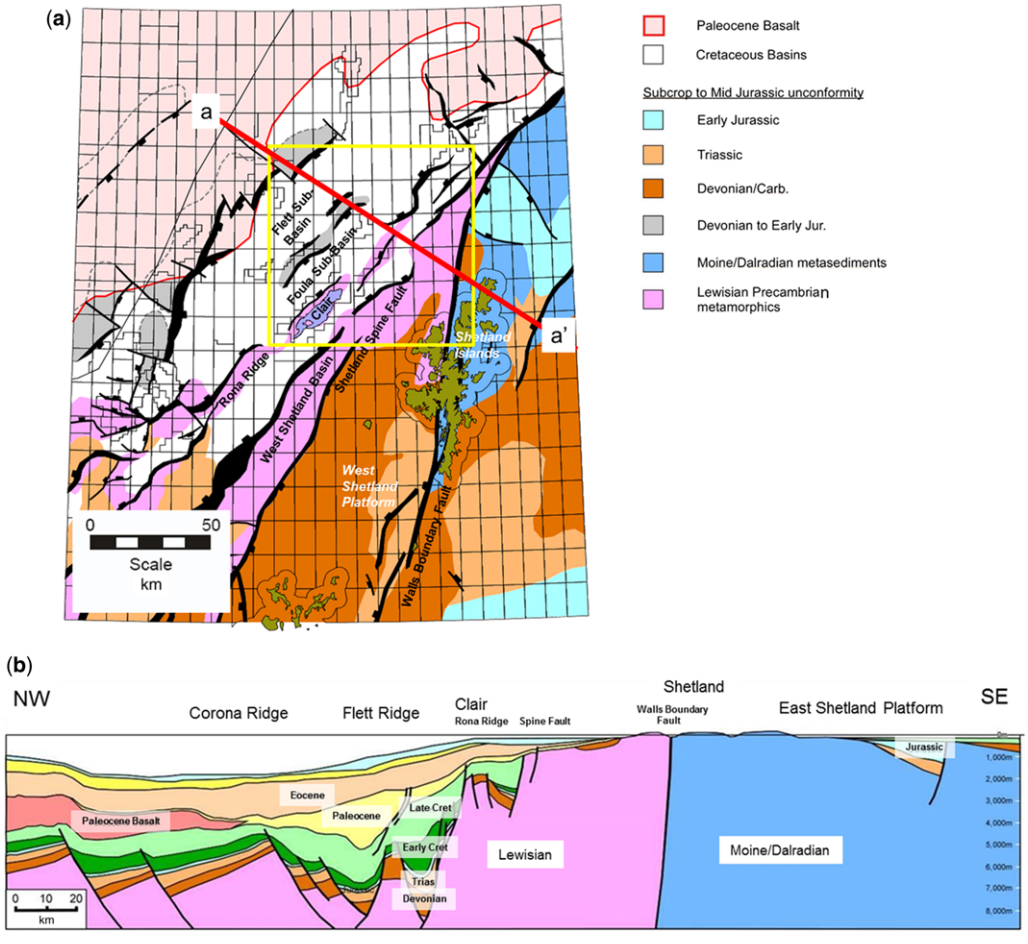

Fig. 4. Clair regional structural setting map and cross-section. Approximate extent of Faroe–Shetland Basin shown by yellow box on map. Location of cross-section shown by a–a′ on map.

Shetland Spine Fault. Displacement may have been transferred between these major faults by north–south-trending transfer faults. In the Early Devonian, accommodation space was created with half-graben geometry, superimposed on a regional fluvial system fed from what is now Greenland (Nichols 2005). This may have resulted from gravitational collapse of the Caledonian orogenic belt (Coward *et al.* 1989; Earle *et al.* 1989). It is unlikely that it is due to the occurrence of a strike-slip pull-apart basin as there are no convincing strike-slip indicators in Clair. It is, however, worth noting that the neighbouring Orcadian Basin is a pull-part basin and that regionally a sinistral transtensional regime is interpreted in the Devonian (Dewey & Strachan 2003).

The Mid- to Late Devonian-aged Lower Clair Group sediments largely post-date rifting and infilled a pre-existing topography. Based on an increase in sediment immaturity and substantial cross-fault thickness changes within constituent units, the Lower Carboniferous Upper Clair Group probably commenced with a renewed phase of rifting, coeval with that elsewhere in the UK (e.g. Fraser & Gawthorpe 1990). Rifting resumed in the Permo-Triassic and the Atlantic Basin proper opened during Jurassic to Early Cretaceous times, continuing into the Tertiary with the onset of seafloor spreading in the Paleocene (Doré *et al.* 1999). Atlantic rifting occurred mainly along NW- or SE-dipping faults. There is significant thickening of Cretaceous sediments in the hanging wall of the NW-dipping Rona Ridge Fault (several kilometres), indicating that this structure accommodated a large amount of the total extension at this time. The SE-dipping Clair Ridge Fault and associated synthetic faults also have large Cretaceous offset (kilometre-scale in total). From the late Paleocene, the Faroe–Shetland Basin began to rapidly subside. However, diagenetic evidence indicates that the Clair area was never deeply buried, and so probably formed a persistent footwall high.

The first reservoir fractures formed during the early tectonic history of the field, perhaps during the collapse of the Caledonian Belt or during subsequent rifting. One or two dominant fracture sets are typically developed, often parallel or perpendicular to nearby faults that pre-date the Base Cretaceous Unconformity (Barr *et al.* 2007, Fig. 3). It is unlikely that this relatively simple fracture pattern can be inverted to elucidate the many stress states likely to have been experienced by Clair since the Devonian. More likely, favourably oriented pre-existing faults and fractures have been reactivated many times during Clair's tectonic history into the Mesozoic and Tertiary. Many fractures and fault zones display evidence of multiple events (e.g. granulation seams cut by parallel brittle fractures, cemented, re-fractured and re-cemented brittle fractures). Evidence from the Clair Phase 1 area shows that fractures that are effective in allowing pressure communication across shales today were ineffective during oil migration (Barr *et al.* 2007), believed to have occurred during the Tertiary. There must therefore have been significant post-rift fracturing events, perhaps related to uplift by the Tertiary Icelandic plume, perhaps to NW–SE Ridge push and Alpine compression.

Field-scale structure relevant for well planning

The most prominent structural feature within the Clair Field closure is the Clair Ridge Fault (Fig. 5). This fault separates the Clair Phase 1 area from the Clair Ridge area with throws of the order of hundreds of metres at basement level. It was clearly active during Devonian and Cretaceous times given the thickness variations across it. The rollover anticline to this fault is called the 'Clair Core' (Fig. 5), with the fault considered to have a listric geometry at depth that soles out within the Clair Basement, perhaps into a relaxed Caledonian thrust (e.g. Coward *et al.* 1989).

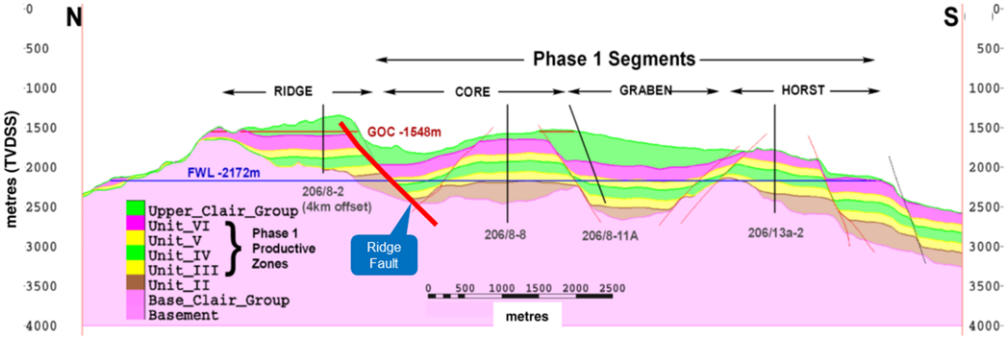

Fig. 5. Cross-section from Clair Ridge to Clair Platform area (modified from Barr *et al.* 2007).

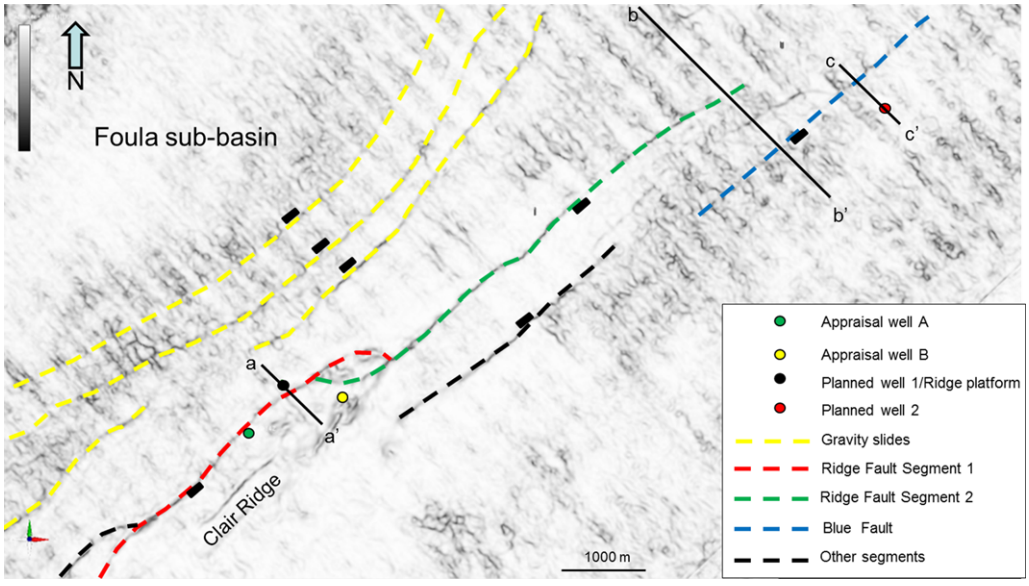

Fig. 6. Coherency map view (at *c.* 570 m TVDSS) in the Tertiary, showing the fault segments and wells discussed in this paper. The seismic data acquisition footprint is evident from top-left to bottom-right of the image.

A map view of the seismic coherency attribute across part of the Clair Field at approximately 570 m total vertical depth subsea (TVDSS) in the Tertiary section (Fig. 6) shows that the Ridge Fault consists of two main segments. Segment 1 is indicated by a dashed red line and segment 2 by a dashed green line in Figure 6. The relay ramp between the segments appears to be breached at various depths in the Tertiary and Cretaceous sections (e.g. just north of the Appraisal Well B in Fig. 6).

Figure 7 shows typical vertical fault segmentation in Clair Field along cross-section b–b′ (Fig. 7a, b) and the evolution of this segmentation using some simple schematic sections (Fig. 7b–d). The Ridge Fault (segment 2; dashed green line in Fig. 6) and the blue fault (also shown in Fig. 6) are mapped with significant displacement at basement level (point 1 in Fig. 7). This progressively decreases upwards and the blue fault changes dip at approximately 1200 m TVDSS, which coincides with the Tertiary/Cretaceous boundary (point 2 in Fig. 7). This geometry may reflect a reactivation of the fault (under slightly different stress field orientation) or simply that there is a change in rock properties from tight muds to porous sandstone, the steeper section of the fault resulting from propagation through material with a higher friction angle. The blue fault has reoriented in strike and dip directions, and then broken down into segments at the boundary. This segmentation and relay ramp formation has created a fault zone wider than that for a single fault surface. The Ridge and blue faults also have associated antithetic faults where the fault changes dip (point 3 in Fig. 7). These observations are important in well planning for deciding the necessary fault standoff. This is the distance that a well should stay away from a fault to avoid the risk of geotechnical problems. If the desire is to avoid drilling through fault-damaged rock, an exclusion zone is defined not just by the width of an individual fault damage zone, but by the aggregate width affected by all the fault splays and their damage zones.

The Ridge and blue faults contain multiple splays, most likely formed as a result of block rotation (Fig. 7). This can be explained be a series of restorations in Figure 7. Figure 7c shows a simple restoration on the Upper Clair Group growth package in the hanging wall of the Ridge Fault, then a Chevron reconstruction (e.g. Fossen 2010) with *c.* 60° antithetic shear flattens the top structure (Fig. 7d). This shear angle has been chosen based upon antithetic faults in the hanging wall of the Ridge Fault that are consistently dipping from 45 to 60° (e.g. black fault within block B, Fig. 7a–c). The Ridge Fault becomes progressively lower angle with Cretaceous block rotation, until new segments break through at mechanically more favourable angles (consistent with an Andersonian model of faulting, e.g. Anderson 1951). The most recent segment of the fault is indicated by the solid green

line in Figure 7b, c. The seismic character of the Ridge Fault wedge (indicated A in Fig. 7a) is very similar to that in the hanging wall of the Ridge Fault (indicated B in Fig. 7a). In particular, the seismic reflectors are less well defined than in the Lower Clair Group (compare the seismic character close to labels A and B with that close to label D in the Lower Clair Group). This suggests that this wedge was part of the overall growth package of the Ridge Fault and provides further evidence for the above model. A further wedge can be observed next to the blue fault in the Lower Cretaceous (indicated C in Fig. 7). This is also suggestive of Late Cretaceous block rotation.

In addition to block rotation, deactivation of early formed SE-dipping faults is favoured by long-wavelength rotation (5–10° to the NW) of the outer continental shelf owing to post-rift thermal subsidence and sediment loading.

Note that the geometry of the basement offset faults is uncertain with depth. The interpretation in Figure 7a allows these faults to detach on Caledonian thrusts, consistent with the Coward *et al.* (1989) model. Also note the presence of arcuate-shaped faults in map view (dashed yellow lines in Fig. 6). These are shallow detachment (Tertiary) gravity slides that are typical in passive margins (e.g. Gluyas & Swarbrick 2004). They are to be expected given the location of the Rona Ridge close to the continental shelf-slope break (Fig. 4b).

Distance to fault in the Tertiary section

During the planning of well 1 (Fig. 6), high-definition seismic data showed that some of the wells were much closer to the Clair Ridge Fault (segment 1 on Fig. 6 and point 3 on Fig. 8a) than previously imaged (Fig. 8a). The original (approximate) mapped location of the Ridge Fault is shown by point 4 in Figure 8a. The new data offered improvement by removal of multiple contamination of the data, which resulted in an improvement in fault definition. Consequently, this well also tracked the fault plane for long distances (hundreds of metres). This was unacceptable as there was a risk of wellbore instability owing to the presence of unconsolidated rock and difficulty in finding competent rock in which to place the casing shoe (indicated on Fig. 8a). Note that the well closest to the fault (i.e. planned well 1 in Fig. 6) with the casing shoe (point 2 on Fig. 8a) cannot be easily straightened out to increase the distance to the fault because it would inevitably collide with future planned wells (as indicated by point 1 in Fig. 8a). The surface location had already been chosen to keep the platform and associated seabed infrastructure inboard of the gravity-driven faults, to avoid drilling multiple wells across the Ridge

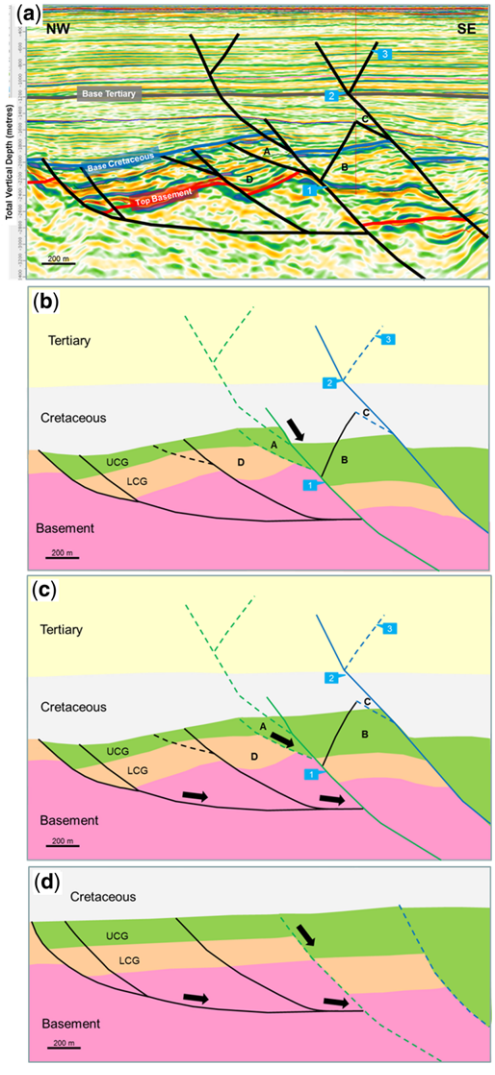

Fig. 7. Listric fault model for Clair Field with (**a**) seismic section (b–b′ in Fig. 6) in dip direction (NW–SE) through Ridge and blue faults showing main structural features relevant for well planning. (**b**) Schematic version of (a). (**d**) Faulting in the Carboniferous resulted in the thickness change of the Upper Clair Group (UCG). Extension along the listric fault during the Cretaceous caused block rotation in (**c**) and new faults formed at mechanically more favourable angles. The UCG now lies in the footwall of the new Ridge Fault. Antithetic faults are required to accommodate the extension. The seismic character in the UCG (labels A and B) is quite different from that in the Lower Clair Group (LCG) (label D), which supports the above model.

Fault and to avoid seabed obstructions (glacial moraines). From a project perspective, risks to the entire facility or to multiple wells rank higher than risks to individual wells. It was therefore necessary to assess and mitigate any risks associated with the close approach of planned well 1 to the fault. This emphasizes the importance of planning the shallow sections of wells on high-resolution seismic data as opposed to data optimized for a much deeper reservoir target.

The key question to be answered was 'what is an acceptable standoff from this fault at this depth?' The workflow used to answer this question involves using a combination of outcrop, seismic and well data. This distance must cater for the lateral uncertainty on the fault position and a potential fault damage zone. The fault has been interpreted through the centre of an inflexion zone (with the edge of the flexure on the purple event indicated on Fig. 8b) that is approximately 50 m wide. It is possible to make reasonable interpretation at the edges of this inflexion up to 25 m from the most likely interpretation (dashed black line in Fig. 8b). This lateral uncertainty also accounts for seismic survey errors and different interpretations of the fault's lateral position by three different seismic interpreters. Given this, the lateral uncertainty on the fault position is ± 25 m.

The potential damage zone width (later referred to as zone of disturbance and inner damage zone/fault core) is indicated by a dashed pink line in Figure 8b. To define the width of this zone, we analysed drilling data for the offset appraisal wells that penetrate the Ridge Fault (Fig. 8c). Appraisal Well A (Fig. 6) penetrates segment 1 of the Ridge Fault in the Tertiary at *c.* 650 m (Fig. 8c). For each well, a 'zone of disturbance' width has been calculated from drilling data. It should be noted that there were no major non-productive time events associated with both these appraisal wells (A and B in Fig. 6) in the respective well sections. The chart in Figure 9 is a collation of logging ROP (rate of

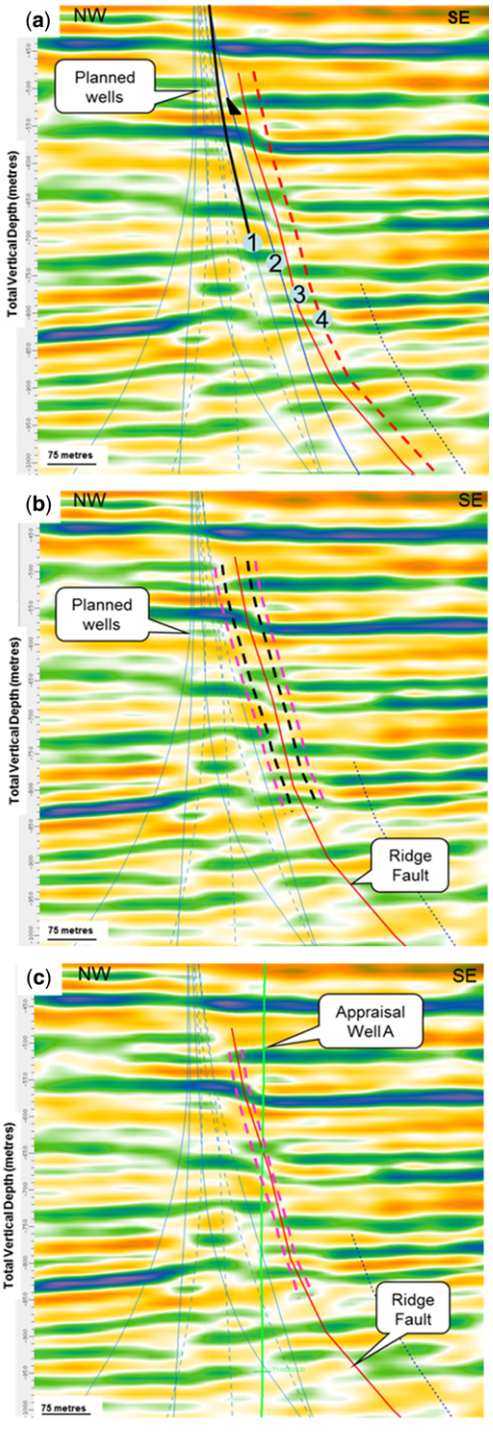

Fig. 8. Seismic sections through an acoustic impedance volume along line a–a′ in Figure 6, showing (**a**) Ridge Fault segment 1 (red, at point 3) imaged closer to planned wells than expected. Casing shoe indicated on well path by black triangle. The closest well, that is, planned well 1 in Figure 6 (at point 2), cannot be straightened out (as shown at point 1) as it would collide with other wells. Also shown is the original mapped position of the fault at point 4. (**b**) Lateral seismic uncertainty (black dashed line) and potential zone of disturbance or inner damage zone/fault core (pink dashed line). (**c**) Appraisal Well A, projected on to section, penetrates segment 1 of the Ridge Fault at *c.* 650 m TVDSS. Dashed pink line shows extent of zone of disturbance or inner damage zone/fault core. Colour scale (acoustic impedance, normal polarity): purple/green denotes a peak = increase in impedance; red/yellow denotes a trough = decrease in impedance.

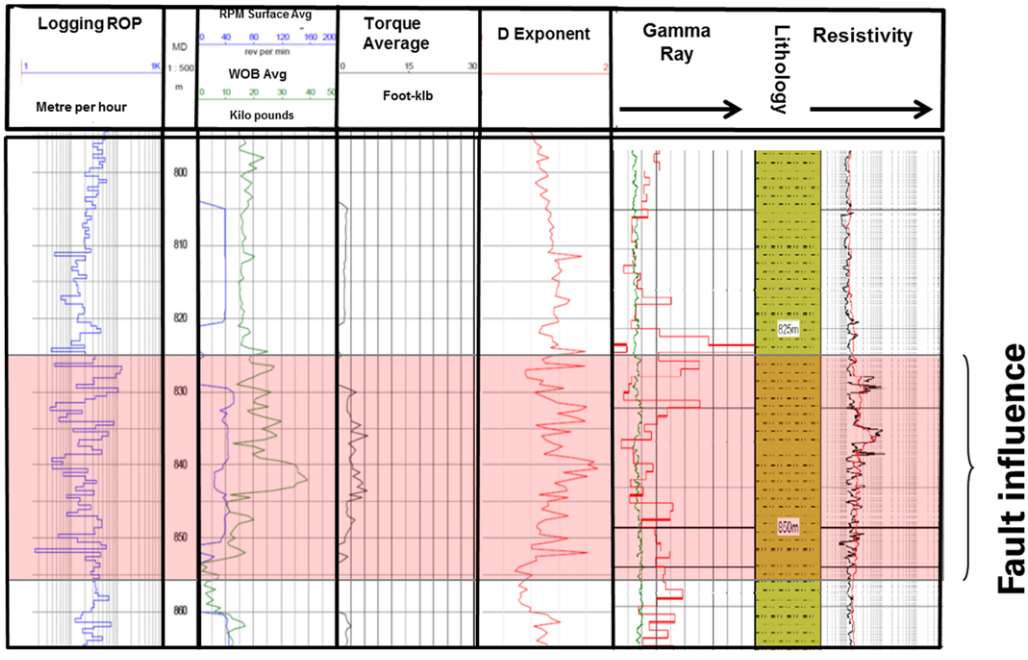

Fig. 9. Drilling data from Appraisal Well A used to define relevant damage zone width. From left to right; logging ROP (rate of penetration in metre per hour), WOB (weight on bit), torque, *D* exponent (a combined 'drillability' indicator) and γ-ray and resistivity logs. The lithology is mainly siltstone.

penetration), WOB (weight on bit), torque, *D* exponent (a combined 'drillability' indicator) and γ-ray and resistivity logs. Each log character takes the form of a bow, marked as fault influence on Figure 9. There is no core in this well to calibrate the resistivity response, but it is picking out either a change in lithology or cemented zone. Geologically, the zone of disturbance is likely to comprise the fault core (consisting of gouge and breccia; e.g. Caine *et al.* 1996) and perhaps the highly deformed inner damage zone, rather than the whole damage zones referred to in some of the literature (e.g. Beach *et al.* 1999). At some point within the outer damage zone, deformation intensity has probably declined to a level where it no longer has an impact on drilling. The 'zone of disturbance' along the well can be used to calculate the relevant fault core/inner damage zone thickness using trigonometry. An example of this is given in Figure 10 for Appraisal Well B (see Fig. 6 for location).

Appraisal Well B, which penetrates the Ridge Fault (segment 2) in the Cretaceous, has a 'zone of disturbance' or fault core/inner damage zone width of 15 m (Fig. 10), whereas Appraisal Well A crosses the fault (segment 1) shallower in the Tertiary and has a 5 m zone of disturbance. This is consistent with a fault losing its displacement upwards towards its tip.

This tells us the point at which we expect fractures to become sufficiently sparse that they no longer have a material impact upon drilling. Given

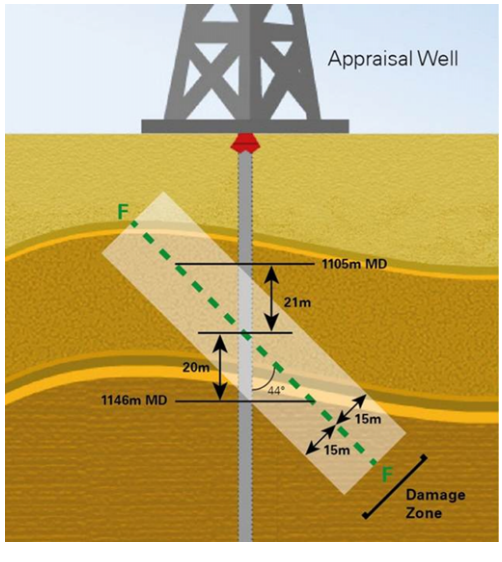

Fig. 10. Determination of fault core/inner damage zone width for Appraisal Well B using trigonometry.

that the planned well (1) is closest to the Ridge Fault segment 1 at *c.* 500 m TVDSS, it is likely that this 'zone of disturbance' or fault core/inner damage zone width will be less than *c.* 5 m at a displacement of approximately 25 m. This is a higher ratio than that in Childs *et al.* (2009, fig. 6), who show that the maximum fault core width for a displacement of 10 m is approximately 1 m in unconsolidated rock. However, the local empirical calibrations described here have more relevance to this problem than predicting the width of the fault core or the outer limit of the damage zone from fault throw as captured in the literature (e.g. Knott 1994; Beach *et al.* 1999; Childs *et al.* 2009).

The geometrical considerations of the fault relay zone indicate that any fault damage is likely to be asymmetrical (from hanging wall to footwall). It is likely to be narrower in the footwall than in the hanging wall as the hanging wall side of the fault contains relay-ramp-associated deformation and the splaying geometries described in the previous section. At the stratigraphic level in the Tertiary shown in Figure 6, the ramp has been breached. However, at other depths in the Tertiary, the two Ridge Fault segments form relay-ramps, illustrating the complexity of the structural evolution of the hanging wall.

Given the lateral uncertainty on the fault ($\pm$25 m), and fault core width of approximately 15 m (to cover the increase in fault displacement with depth), the standoff distance is approximately 40 m. It was not possible to achieve this standoff along the entire length of the well in the top section. However, planning the well outside of this standoff distance for most of its length significantly reduced the geotechnical risk to wellbore and casing shoe placement.

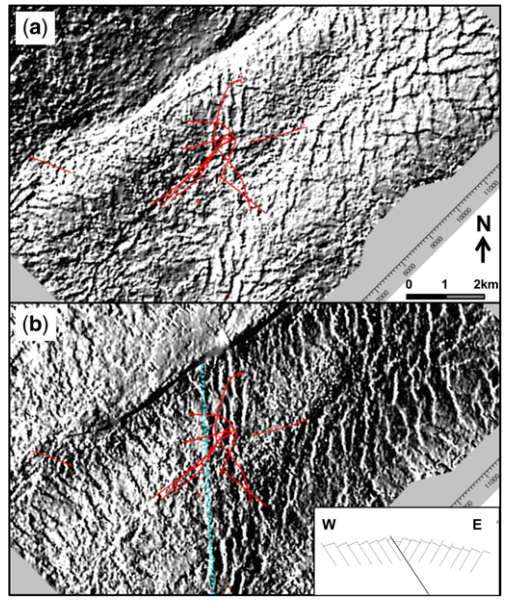

Fig. 11. Polygonal faulting highlighted by shaded illumination of a mid-Maastrichtian seismic depth map. (**a**) Illuminated from the SE (narrow segments are fault planes, broad segments are bedding planes). (**b**) Illuminated from the west to highlight the polarity flip in north–south polygonal faults across an underlying tectonic fault (blue trace). The inset schematically represents the polarity flip. Selected appraisal and development wells are shown in red and the scale is in metres.

Polygonal faulting in the Cretaceous section

The Clair Cretaceous mudstones are sufficiently weak that wellbore stability is primarily driven by rock strength rather than pore pressure and fracture gradient. The failed wells listed in Narayanasamy *et al.* (2009, fig. 4) were drilled in a part of the field where pore pressure lies between 1.0 and 1.1 sg, yet 1.5–1.6 sg mud weight was required to stabilize high-angle wells. That is more than was predicted using a conventional wellbore stability model calibrated to appraisal wells that were typically near-vertical in this hole section. Polygonal faulting was considered as a potential cause of instability. High-angle wells must cross more faults and it is difficult to avoid drilling fault-parallel at some point, potentially exposing a long, brecciated section.

Polygonal faulting is commonly developed in mudstone sequences during early burial and diagenetic processes (see Cartwright & Dewhurst 1998; Goulty & Swarbrick 2005 for details). The Cretaceous-age section above the Clair Field contains a typical, polygonal fault pattern (Fig. 11), with increased polygon size in the SE where the stratigraphic interval is thicker. A preferred alignment and polarity of the faults is seen on the crest of the Clair Phase 1 structure (the red wells on Fig. 11), symmetrical about an underlying north–south tectonic fault over which the mudstones are draped (inset in Fig. 11b). This imparts a regional dip to the overlying mudstones and the polygonal faults dip preferentially upslope. Similar alignment has been observed at a larger scale on regional anticlines and passive margins (e.g. Cartwright & Dewhurst 1998; Stuevold *et al.* 2003). The tectonic fault extends into the polygonal-faulted interval so tectonic as well as gravitational stresses may have influenced small-scale fault development (compare the switch from polygonal to radial faulting around salt diapirs described by Davison *et al.* (2000) and Stewart (2006)). In the area of the Ridge platform (north of the blue fault trace), this sequence is

largely eroded and too thin for the presence or absence of polygonal faults to be resolved.

Early attempts at extended-reach drilling in Clair were hampered by wellbore instability in Upper Cretaceous mudstones (Narayanasamy *et al.* 2009). This had not been expected based on drilling performance in vertical and mildly deviated wells and was determined to result primarily from mudstone mechanical anisotropy. Rock strength varies by up to a factor of 4 depending on the angle to bedding at which it is measured (Narayanasamy *et al.* 2009). The Clair observations are best matched by a model with a high vertical to horizontal stress ratio (based on multiple leak-off tests and one extended leak-off recording fracture propagation and subsequent closure) and a low horizontal stress anisotropy (based on a similar mud weight being required irrespective of well azimuth). Significant overpressure can be ruled out based on observations made in vertical wells drilled with low mud weights. Under these circumstances, and given mechanically weak rocks, well inclination becomes the dominant factor (a horizontal wellbore is exposed to the vertical to horizontal stress ratio, a horizontal well to the $S_{H\max}$ to $S_{H\min}$ ratio). An additional factor is the intersection angle between the wellbore and bedding. The Clair mudstones are at their weakest when tested at about 60° to the bedding normal (Narayanasamy *et al.* 2009). Once identified, this failure mechanism can be numerically modelled using either a fully anisotropic (orthotropic) model or one where the weakest orientation is interpreted as controlled by weak bedding planes represented by a well-established plane-of-weakness theory (e.g. Jaeger *et al.* 2007). With the generally low bedding dips encountered (typically $<10°$), the result is a sharp increase in the mud weight required to stabilize a well deviated at 45° from the vertical compared with one within 15° of vertical (Narayanasamy *et al.* 2009, fig. 13). The required mud weight also depends on bedding dip (Narayanasamy *et al.* 2009, fig. 15) and the intersection angle between wellbore and bedding.

Suitably calibrated, this weak-plane model provides a good match to Clair drilling data. The properties of the weak planes were initially defined empirically then refined using laboratory tests conducted on Cretaceous mudstone core collected in a Clair Phase 1 development well (Narayanasamy *et al.* 2009). This mudstone core also provides an opportunity to assess the potential contribution of polygonal faulting to wellbore instability. Cores were cut in two intervals, Maastrichtian and Campanian (Fig. 12), in a location observed to be free of seismically identified faulting. Nevertheless, each approximately 25 m core contained one fault and its associated damage zone.

The Maastrichtian fault dips at a high angle to bedding (*c.* 60°), which itself dips at about 15°, and comprises a 0.5 m-thick fault core (largely calcite cemented), and a damage zone with 1–2 m half-width comprising glossy shear fractures with occasional lenses of scaly claystone (Fig. 12a). The calcite cement could imply that the fault acted as a conduit for fluid flow (cf. Berndt *et al.* 2003). However, the host mudstones contain substantial amounts of coccolith-derived material and carbonate concretions or stringers, so local remobilization of calcite during diagenesis is also possible. This fault zone is reasonably well consolidated, so although a small amount of loose material could fall into an open wellbore, it is only likely to pose a significant problem where the fault is exposed in a long section of wellbore (i.e. where the well is drilled subparallel to a fault). If cementation is patchy, other faults or other parts of this fault could be much weaker. Unfortunately, the pervasive nature and random orientation of polygonal faulting mean that in practice most wells drilled close to the fault dip angle of 45–60° will be exposed for some part

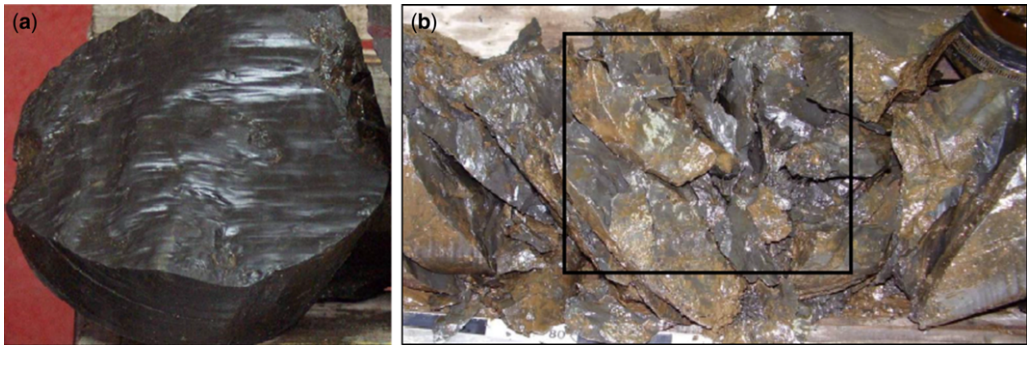

Fig. 12. (**a**) High-angle fault zone dipping *c.* 60° to bedding in Maastrichtian mudstone (0.5 m fault breccia, 1.5 m hanging wall damage zone). The core is *c.* 20 cm wide. (**b**) Bed-parallel shear zone in Campanian mudstones; the damage zone contains several fault breccias, each tens of centimetres thick.

of their length. Although not specifically identified as a root cause, it is likely that some of the instability seen in such wells is fault related. The infall of loose material cannot be prevented by increasing mud weight and has to be managed by drilling practices: the role of the structural geologist is to identify the polygonal faulted intervals and their likely fault plane dips, so that the drilling engineer can be informed and prepared. On seismic data, the Maastrichtian is the most obviously polygonal-faulted interval in Clair.

The Campanian fault comprises a bed-parallel shear zone containing claystone breccia (lenses of foliated/scaly clay and clasts of wall-rock, Fig. 12b) and slickensided shear surfaces. The fault core is about 2 m wide and the damage zone 10 m wide or more (it extends to the base of the core, although with diminished intensity). This would be a challenging interval to drill subparallel to bedding and the weak-plane model would predict problems from about 45° (a lower strength would be input for a bed-parallel fault than for conventional bedding). Seismic data do not reveal polygonal faulting in the Campanian at this location. However, it lies at the base of the Maastrichtian polygonal fault tier so may represent a basal detachment to that system. The cored well (Fig. 12) lies in the region of Figure 13 where faults have a preferred orientation and polarity, implying a net shear displacement that may increase the intensity of deformation relative to a conventional polygonal fault system. A similar effect might be expected where polygonal fault systems are systematically aligned on continental slopes, perhaps augmented by activation of this weak zone during gravitational sliding (cf. McClay *et al.* 2003).

In addition to directly generating inherently weak rocks, polygonal faulting can also impact wellbore stability through bed rotation. The Clair polygonal faults typically rotate bedding by about 15°. The sensitivity of conventional bedding-plane failure to wellbore intersection angle means that this can either be favourable for stability in deviated wells (beds dip against the well direction) or unfavourable (beds dip in the well direction). Image logs were acquired in a number of Clair wells to identify bedding and fault dips. Two examples are shown in Figure 13. In Figure 13a, bed rotation owing to polygonal faulting is generally favourable to wellbore stability; in Figure 13b it is unfavourable. In some places it is possible to predict a consistent bed rotation from seismic observations; in others the sense of rotation is random or below seismic resolution. In those cases, a judgement must be made on whether to model wellbore stability assuming an average dip based on the seismic envelope, or to allow for a range of favourable and unfavourable rotations. In general it is prudent to consider the possibility that some combination of subseismic faulting, bed rotation and inherently weak fault rocks will make some sections of a wellbore unstable, regardless of the predictions from a coarse model built using generalized bedding dips. In situations where polygonal faulting is known or expected and bedding-plane failure is a contributor to wellbore instability, it is important to obtain image logs or other bedding-dip indicators in order to verify actual bedding–wellbore intersection angles and properly calibrate predictive models.

Casing shoe placement and structural model in the Cretaceous section

An issue relating to casing shoe placement was identified during the planning of Well 2 (cross-section c–c′, Fig. 6). Ideally, this appraisal well should occupy a more crestal location than planned (Fig. 14). This is to maximize the exposure to the hydrocarbon column. However, shoe placement would be very challenging in the highly faulted structural crest. The green fault in Figure 14 is the original fault which upon rotation became inactivated and the conditions were then right for the younger blue fault to form (which is also shown in Fig. 6). This is consistent with the model discussed in the field-scale structure relevant for well planning section.

Planned Well 2 (vertical black line in Fig. 14 and red dot in Fig. 6) will still intersect these faults but will do so where the horizon tops do not coincide with the faults. That way, horizons can be identified with confidence during drilling allowing for easier operational decisions. For example, the 9-5/8" casing shoe (in the Santonian section in Fig. 14) is planned to be set in a relatively structurally benign area (i.e. away from the black–green fault intersection at the Campanian–Santonian boundary). It will also enable calibration of seismic tops for depth conversion, to the benefit of the structural model, and avoid intersecting faults around the Upper–Lower Maastrichtian boundary. Biostratigraphic dating of cavings from previous wells (some of the failed wells referred to in Narayanasamy *et al.* 2009) showed persistent dates from around this boundary, indicating that those rocks are particularly weak, probably weaker than those in the cored intervals. It was deemed prudent to avoid drilling that interval where it might have been further weakened by faulting.

Fault seal in reservoir section

Pressure prognosis has important implications for well design. For example, a new well drilled into a neighbouring fault block to one occupied by

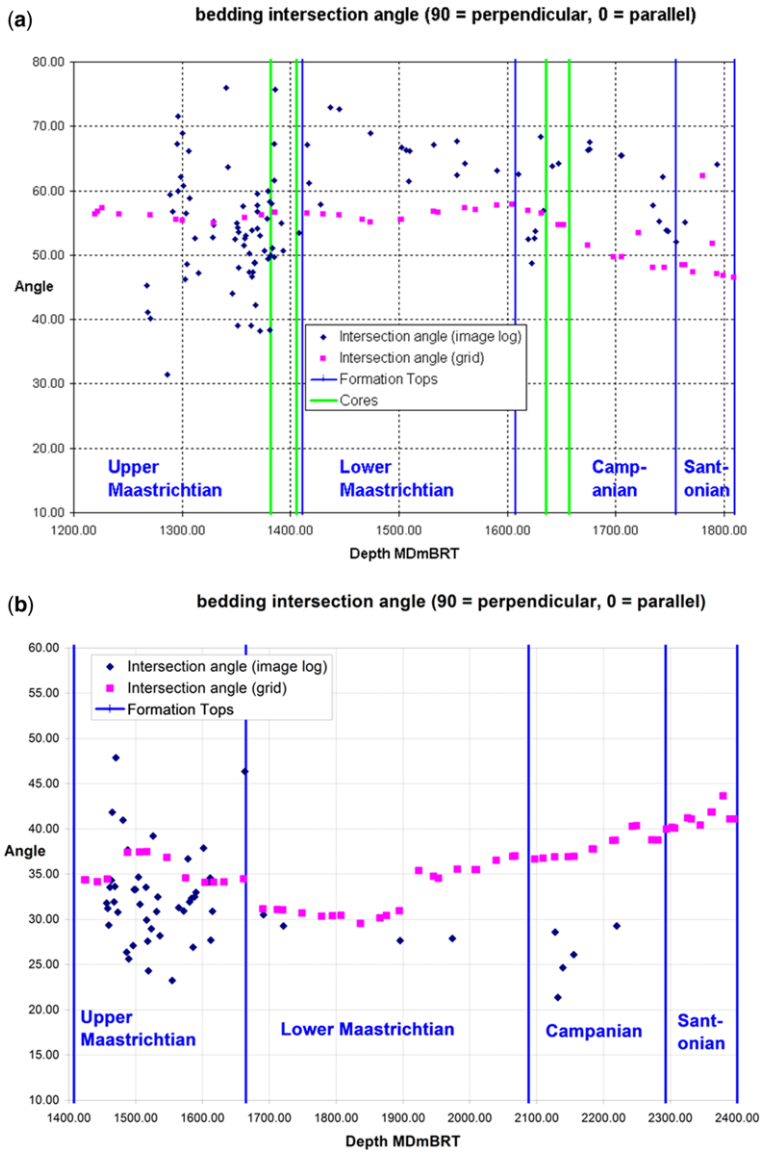

Fig. 13. Intersection angle (in degrees) of bedding with two deviated wellbores, as observed on image logs and gridded from an enveloping seismic surface (90° would be perpendicular, 0° parallel). (**a**) Polygonal faulting has mostly rotated bedding favourably for wellbore stability (closer to perpendicular to the wellbore, except in the Upper Maastrichtian). Cavings were observed from the Upper Maastrichtian section but controlled by increasing the mud weight. See also cored well in Figure 12. (**b**) Polygonal faulting has mostly rotated bedding unfavourably for wellbore stability (closer to parallelism with the wellbore). This well was a sidetrack of a hole section that had been lost owing to wellbore instability, with most cavings dated to the Upper Maastrichtian. The sidetrack was drilled with significantly increased mud weight and was stable.

an existing production well may not be at virgin pressure. This is because the block-bounding fault(s) may not be fully sealing on a production timescale. Therefore, in order to complete a pressure prognosis for a planned well, judgement is required by a geologist on the nature of the juxtaposition and fault rock sealing capacity across such a fault on a production timescale. The example in Figure 15 shows that the targeted younger sands in Block 2 are in contact with older sands

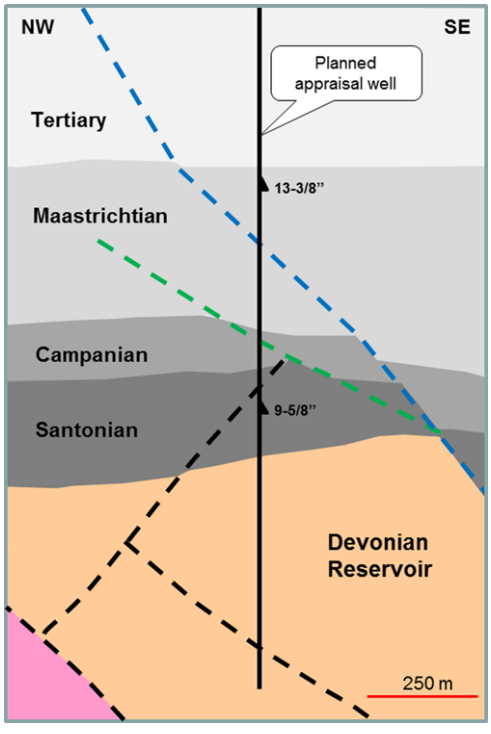

Fig. 14. Schematic section (c–c′ in Fig. 6) illustrating the faulted geometry along the well path of planned Well 2 with implications for well planning and casing shoe placement. Vertical:horizontal scale is 1:1.

in Block 1 across a normal fault. Fault seal cannot be predicted using clay content algorithms, for example shale/gouge ratio (e.g. Yielding *et al.* 2010) and shale smear factor (e.g. Lindsay *et al.* 1993), as these sands have low clay content. Therefore, judgement has to be made based upon burial/diagenetic history and potential for cataclasis and authigenic cement to create a sand-on-sand seal (e.g. Gibson 1998; Fisher *et al.* 2003; Fisher & Jolley 2007). In this case, the initial depth of burial is not considered to be sufficient to produce structures other than disaggregation or granulation seams that have poor sealing potential relative to clay-rich or quartz-cemented fault rocks (Fisher & Knipe 1998; Ogilvie & Glover 2001). It is also observed in the Devonian sandstones that the deformation bands that form early during burial are cross-cut by open fractures, which reduces their sealing potential.

In Block 1, the amount of depletion since the production well start-up was calculated from the difference between virgin pressure and actual pressures. This was used to predict the expected maximum depletion at spud date for the planned well in Block 2. A probability was assigned to this depletion case in Block 2 based upon well performance, other dynamic factors and distance of the new well from the existing well. This was then combined with the juxtaposition analyses which indicate that communication between the two blocks is geologically possible in the first place.

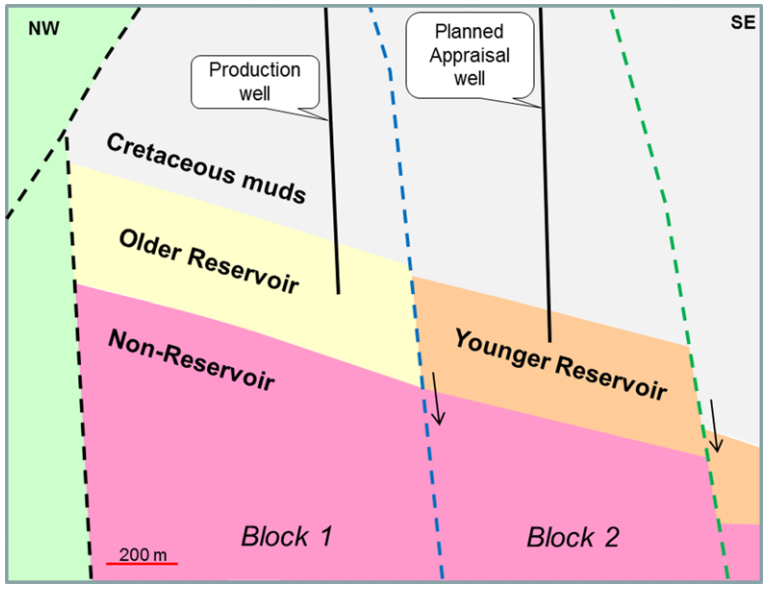

Fig. 15. Juxtaposition of Devonian sandstones in block containing production well (Block 1) against younger sandstones in Block 2, containing planned well. Vertical exaggeration is 2.5×.

Conclusions

Structural geology has a significant contribution to well planning in a hydrocarbon field. Examples from the Clair Field in the West Shetland Basin have been given in this paper. These have been discussed in three well sections: top (Tertiary), middle (Cretaceous) and reservoir (Devonian/Carboniferous). Specifically:

- *Distance to fault in Tertiary section* – judgement on the expected fault geometry (seismic imaging – related position uncertainty, inner fault damage zone/fault core/zone of disturbance width and fault geometries) is required in order to justify the well target standoff distance to a seismically mapped fault or faults. This work has also integrated appraisal well drilling data including rates of penetration, resistivity logs and weight on bit information. The two appraisal wells penetrate the Clair Ridge Fault at different depths and the zone of disturbance is narrower with the shallower penetration. This is to be expected as the fault loses its displacement towards it tip.
- *Polygonal faulting in Cretaceous section* – rock strength anisotropy present in the mudstone makes wellbore stability dependent on bedding dip and wellbore-to-bedding intersection angle, as well as on the more usual controls of well inclination, pore pressure and fracture gradient. Faults may pose challenges for wellbore stability either directly, through infall of unconsolidated fault breccia, or indirectly, by rotating bedding to an adverse angle. The structural geologist should be involved in characterizing polygonal faults to inform drilling engineering plans.
- *Casing shoe placement and structural model in Cretaceous section* – an understanding of the structural evolution of the overburden section of the well is critical to well placement, especially if the seismic data quality is poor. The example given in this paper illustrates a well placement slightly down-dip from that originally anticipated in order to avoid complex fault intersections, consistent with the fault block rotation structural model.
- *Fault seal in reservoir section* – when planning infill wells within a producing oilfield, judgement on the nature of the reservoir juxtaposition across a fault and the effective permeability of its fault gouge is necessary. This is to accurately predict pore pressures in virgin fault blocks, adjacent to fault blocks that already contain production wells. The fault planes discussed here do not have sufficient offsets to bring significant amounts of mudstone into the fault plane and are dominated by sand-on-sand contacts and sandy fault gouge that have not been deeply buried. That makes them inherently baffling to flow rather than sealing.

References

Anderson, E. M. 1951. *The Dynamics of Faulting*. Oliver & Boyd, Edinburgh.

Barr, D., Savory, K. E., Fowler, S. R., Arman, K. & McGarrity, J. P. 2007. Pre-development fracture modelling in the Clair field, west of Shetland. *In*: Lonergan, L., Jolly, R. J. H., Rawnsley, K. & Sanderson, D. J. (eds) *Fractured Reservoirs*. Geological Society, London, Special Publications, **270**, 205–225, http://dx.doi.org/10.1144/GSL.SP.2007.270.01.14

Beach, A., Welbon, A. I., Brockbank, P. J. & McCallum, J. E. 1999. Reservoir damage around faults: outcrop examples from the Suez rift. *Petroleum Geoscience*, **5**, 109–116, http://dx.doi.org/10.1144/petgeo.5.2.109

Berndt, C., Bünz, S. & Mienert, J. 2003. Polygonal fault systems on the mid-Norwegian margin: a long-term source for fluid flow. *In*: Van Rensbergen, P., Hillis, R. R., Maltman, A. J. & Morley, C. K. (eds) *Subsurface Sediment Mobilization*. Geological Society, London, Special Publications, **216**, 283–290, http://dx.doi.org/10.1144/GSL.SP.2003.216.01.18

Caine, J. S., Evans, J. P. & Forster, C. B. 1996. Fault zone architecture and permeability structure. *Geology*, **24**, 1025–1028.

Cartwright, J. A. & Dewhurst, D. N. 1998. Layer-bound compaction faults in fine-grained sediments. *Geological Society of America Bulletin*, **110**, 1242–1257.

Childs, C., Manzocchi, T., Walsh, J. J., Bonson, C. G., Nicol, A. & Schopfer, M. P. J. 2009. A geometric model of fault zone and fault rock thickness variations. *Journal of Structural Geology*, **31**, 117–127.

Coney, D., Fyfe, T. B., Retail, P. & Smith, P. J. 1993. Clair appraisal: benefits of a cooperative approach. *In*: Parker, J. R. (ed.) *Petroleum Geology of Northwest Europe: Proceedings of the 4th Conference*. Geological Society, London, 1409–1420, http://dx.doi.org/10.1144/0041409

Cosgrove, J. W. 1998. The role of structural geology in reservoir characterisation. *In*: Coward, M. P., Daltaban, T. S. & Johnson, H. (eds) *Structural Geology in Reservoir Characterisation*. Geological Society, London, Special Publications, **127**, 1–13, http://dx.doi.org/10.1144/GSL.SP.1998.127.01.01

Coward, M. P., Enfield, M. A. & Fisher, M. W. 1989. Devonian basins of Northern Scotland: extension and inversion related to Late Caledonian–Variscan tectonics. *In*: Cooper, M. A. & Williams, G. D. (eds) *Inversion Tectonics*. Geological Society, London, Special Publications, **44**, 275–308, http://dx.doi.org/10.1144/GSL.SP.1989.044.01.16

Davison, I., Alsop, I. *et al.* 2000. Geometry and late-stage structural evolution of Central Graben salt diapirs, North Sea. *Marine and Petroleum Geology*, **17**, 499–522.

Dewey, J. F. & Strachan, R. A. 2003. Changing Silurian–Devonian relative plate motion in the Caledonides: sinistral transpression to sinistral transtension.

Journal of the Geological Society, London, **160**, 219–229, http://dx.doi.org/10.1144/0016-764902-085

Doré, A. G., Lundin, E. R., Jensen, L. N., Birkeland, Ø., Eliassen, P. E. & Fichler, C. 1999. Principal tectonic events in the evolution of the Northwest European Atlantic margin. *In*: Fleet, A. J. & Boldy, S. A. R. (eds) *Petroleum Geology of Northwest Europe*: *Proceedings of the 5th Conference*. Geological Society, London, 41–61, http://dx.doi.org/10.1144/0050041

Earle, M. M., Jankowski, E. J. & Vann, I. R. 1989. Structural and stratigraphic evolution of the Faeroe–Shetland Channel and Northern Rockall trough. *In*: Tankard, A. J. & Balkwill, H. R. (eds) *Extensional Tectonics, Stratigraphy of the North Atlantic Margins*. American Association of Petroleum Geologists, Memoirs, **46**, 461–470.

Fisher, Q. J. & Jolley, S. J. 2007. Treatment of faults in production simulation models. *In*: Jolley, S. J., Barr, D., Walsh, J. J. & Knipe, R. J. (eds) *Structurally Complex Reservoirs*. Geological Society, London, Special Publications, **292**, 219–233, http://dx.doi.org/10.1144/SP292.13

Fisher, Q. J. & Knipe, R. J. 1998. Fault sealing processes in siliciclastic sediments. *In*: Jones, G., Fisher, Q. J. & Knipe, R. J. (eds) *Faulting, Fault Sealing and Fluid Flow in Hydrocarbon Reservoirs*. Geological Society, London, Special Publications, **147**, 117–135, http://dx.doi.org/10.1144/GSL.SP.1998.147.01.08

Fisher, Q. J., Casey, M., Harris, S. D. & Knipe, R. J. 2003. The fluid flow properties of faults in sandstone: the importance of temperature history. *Geology*, **31**, 965–968.

Fossen, H. 2010. *Structural Geology*, 1st edn. Cambridge University Press, Cambridge.

Fossen, H., Schultz, R., Shipton, Z. & Mair, K. 2007. Deformation bands in sandstone – a review. *Journal of the Geological Society London*, **164**, 755–769, http://dx.doi.org/10.1144/0016-76492006-036

Fraser, A. J. & Gawthorpe, R. L. 1990. Tectono-stratigraphic development and hydrocarbon habitat of the Carboniferous in northern England. *In*: Hardman, R. F. P. (ed.) *Tectonic Events Responsible for Britain's Oil and Gas Reserves*. Geological Society, London, Special Publications, **55**, 49–86, http://dx.doi.org/10.1144/GSL.SP.1990.055.01.03

Gabrielsen, R. H. & Koestler, A. G. 1987. Description and structural implications of fractures in late Jurassic sandstones of the Troll Field, northern North Sea. *Norsk Geologisk Tidsskrift*, **67**, 371–381.

Gibson, R. G. 1998. Physical character and fluid-flow properties of sandstone-derived fault zones. *In*: Coward, M. P., Daltaban, T. S. & Johnson, H. (eds) *Structural Geology in Reservoir Characterization*. Geological Society, London, Special Publications, **127**, 83–97, http://dx.doi.org/10.1144/GSL.SP.1998.127.01.07

Gluyas, J. & Swarbrick, R. 2004. *Petroleum Geoscience*. Blackwell, Oxford.

Goulty, N. R. & Swarbrick, R. E. 2005. Development of polygonal fault systems – a test of hypotheses. *Journal of the Geological Society, London*, **162**, 587–590, http://dx.doi.org/10.1144/0016-764905-004

Jaeger, J. C., Cook, N. G. W. & Zimmerman, R. W. 2007. *Fundamentals of Rock Mechanics*, 4th edn. Blackwell, Oxford.

Knott, S. D. 1994. Fault zone thickness v. displacement: results from Permo-Triassic sandstone outcrops in NW England. *Journal of the Geological Society, London*, **151**, 17–25, http://dx.doi.org/10.1144/gsjgs.151.1.0017

Lindsay, N. G., Murray, F. C., Walsh, J. J. & Watterson, J. 1993. Outcrop studies of shale smears on fault surfaces. *In*: Flint, S. S. & Bryant, I. D. (eds) *The Geological Modelling of Hydrocarbon Reservoirs and Outcrop Analogues*. International Association of Sedimentologists, Special Publications, **15**, 113–123.

McClay, K., Dooley, T. & Zamora, G. 2003. Analogue models of delta systems above ductile substrates. *In*: Van Rensbergen, P., Hillis, R. R., Maltman, A. J. & Morley, C. K. (eds) *Subsurface Sediment Mobilization*. Geological Society, London, Special Publications, **216**, 411–428, http://dx.doi.org/10.1144/GSL.SP.2003.216.01.27

Narayanasamy, R., Barr, D. & Milne, A. 2009. Wellbore instability predictions within the Cretaceous mudstones, Clair field, west of Shetlands. Society of Petroleum Engineers, Papers, 124464.

Nichols, G. J. 2005. Sedimentary evolution of the Lower Clair Group, Devonian, West of Shetland: climate and sediment supply controls on fluvial, aeolian and lacustrine deposition. *In*: Doré, A. G. & Vining, B. A. (eds) *Petroleum Geology: North-West Europe and Global Perspectives*: *Proceedings of the 6th Petroleum Geology Conference*. Geological Society, London, 957–967, http://dx.doi.org/10.1144/0060957

Ogilvie, S. R. & Glover, P. W. J. 2001. The petrophysical properties of deformation bands in relation to their microstructure. *Earth and Planetary Science Letters*, **193**, 129–142.

Stewart, S. 2006. Implications of passive salt diapir kinematics for reservoir segmentation by radial and concentric faults. *Marine and Petroleum Geology*, **23**, 843–853.

Stuevold, L. M., Faerseth, R. B., Arnesen, L., Cartwright, J. & Möller, N. 2003. Polygonal faults in the Ormen Lange Field, Møre Basin, offshore Mid Norway. *In*: Van Rensbergen, P., Hillis, R. R., Maltman, A. J. & Morley, C. K. (eds) *Subsurface Sediment Mobilization*. Geological Society, London, Special Publications, **216**, 263–281, http://dx.doi.org/10.1144/GSL.SP.2003.216.01.17

Witt, A. J., Fowler, S. R., Kjelstadli, R. M., Draper, L. F., Barr, D. & McGarrity, J. P. 2010. Managing the start-up of a fractured oil reservoir: development of the Clair field, West of Shetland. *In*: Vining, B. A. & Pickering, S. C. (eds) *Petroleum Geology: From Mature Basins to New Frontiers*: *Proceedings of the 7th Petroleum Geology Conference*. Geological Society, London, 299–313, http://dx.doi.org/10.1144/0070299

Yielding, G., Bretan, P. & Freeman, B. 2010. Fault seal calibration; a brief review. *In*: Jolley, S. J., Fisher, Q. J., Ainsworth, R. B., Vrolijk, P. J. & Delisle, S. (eds) *Reservoir Compartmentalization*. Geological Society, London, Special Publications, **347**, 243–255, http://dx.doi.org/10.1144/SP347.14